Accepted Manuscript

Structural and thermal investigations of Sr_2WO_5

Meera Keskar, S.K. Sali, B.G. Vats, R. Phatak, K. Krishnan, S. Kannan

PII: S0925-8388(16)33871-3

DOI: 10.1016/j.jallcom.2016.11.388

Reference: JALCOM 39885

To appear in: *Journal of Alloys and Compounds*

Received Date: 28 September 2016

Revised Date: 21 November 2016

Accepted Date: 27 November 2016

Please cite this article as: M. Keskar, S.K. Sali, B.G. Vats, R. Phatak, K. Krishnan, S. Kannan, Structural and thermal investigations of Sr_2WO_5, *Journal of Alloys and Compounds* (2016), doi: 10.1016/j.jallcom.2016.11.388.

Structural and thermal investigations of Sr_2WO_5

Meera Keskar*, S.K. Sali, B.G. Vats, R. Phatak, K. Krishnan, S. Kannan

Fuel Chemistry Division, BARC, Mumbai 400085, India

Abstract

The crystal structure of Sr_2WO_5 has been refined using powder X-Ray diffraction (XRD) and neutron diffraction (ND) data. The corner connected WO_6 octahedra forms infinite cis-bridged chains along b axis which are further connected by the layer of Sr atoms to give a three dimensional network. Thermogravimetric study revealed that Sr_2WO_5 on storage picks up moisture from the surrounding to give a mixutre of $Sr(OH)_2$ and $SrWO_4$. Percentage of $Sr(OH)_2$ in Sr_2WO_5 increases with increase of storage time under normal atmospheric condition. The hydrated compound on heating up to 1473 K again yield back Sr_2WO_5. High Temperature X-ray Diffraction (HTXRD) studies of Sr_2WO_5 and $SrWO_4$ in vacuum showed positive thermal expansion in the temperature range of 298–1273 K. Thermogram of Sr_2WO_5 recorded with Differential Scanning Calorimeter (DSC) showed a reversible phase transition at 423 K. Specific heat capacity of Sr_2WO_5 was measured between temperature 463 to 863 K using heat flux DSC.

Keywords : Alkaline earth tungstates; Powder X-ray diffraction; Thermogravimetric analysis; structure; Thermal expansion; Heat capacity

---

* Corresponding author

Email address: mskeskar@barc.gov.in (M. Keskar)

1. Introduction

Tungstates, especially alkaline earth tungstates are very interesting class of materials because of their potential applications in various fields [1-8]. The structural studies of alkali and alkaline earth tungstates revealed the possibility of doping various cations in the host matrices for laser applications. Among these tungstates, schellite structured MWO_4 (M=Ca, Sr, and Ba) have numerous industrial applications in quantum electronics, medical field, X-ray phosphors, cryogenic detectors, catalyst and electron spin resonance studies, in addition to host materials for laser. [9]. There are several reports on photoluminescence studies of rare earth doped MWO_4 systems. [2, 10-12]. MWO_4 compounds are also being used as promising materials for microwave substrate applications [13]. High pressure studies of MWO_4 compounds have been carried and phase transitions in them were discovered using techniques like Raman spectroscopy and Synchrotron X-ray diffraction [14-17].

The phase equilibrium in SrO-WO_3 system is summarized by Grivel and Norby [18]. In this system, they have reported the formation of $SrWO_4$, Sr_2WO_5 and Sr_3WO_6 phases at 1073 K. Structural and thermal properties of $SrWO_4$ and Sr_3WO_6 phases are well studied and reported in literature. Crystal structure of $SrWO_4$ has been carried out by Gurmen et al. using neutron diffraction data [19]. Study on the growth and thermal properties of $SrWO_4$ single crystal has been reported by Fan et al. [7]. They have also measured the thermal expansion and specific heat capacity of the compound using dilatometer and DSC techniques, respectively. Raman study on the pressure induced structural phase transitions in $SrWO_4$ has been reported by Christofilos et al. [20]. Study on the phonon properties of $SrWO_4$ has been reported by Goel et al. [21]. The effects of alkali metal and alkaline earth metal impurities on the synthesis of pure $SrWO_4$ and the stability of this compound under the influence of a humid atmosphere and water have been reported by Krazmanc et al. [13]. They have mentioned that materials having significant tendency to react with the moisture are not a good materials for the applications in electronics, because of the deterioration of their properties in the presence of a moist atmosphere. Recently, the structural and vibrational properties of $SrWO_4$ have been studied by angle dispersive synchrotron X-ray diffraction and Raman spectroscopy measurements and four polymorphs of the compound were confirmed [14]. Detailed study on structural phase transitions of Sr_3WO_6 at different temperatures, has been carried out by King et al. using electron diffraction, synchrotron

X-ray powder diffraction and neutron diffraction techniques [8]. Enthalpies, entropies and the standard Gibbs energies of formations of Sr_3WO_6, Sr_2WO_5 and $SrWO_4$ have been calculated by Levitski and Scolis using electrochemical cells [22]. During the luminescence study of double perovskite structured Sr_3WO_6:K^{1+} doped with Eu^{3+}, an intense red emission was observed by Zhao et al. [23]. In Sr_2WO_5 compound, only luminescence study has been carried out. Blasse and Heuvel [24] have reported that at low temperature, Sr_2WO_5 when activated with hexavalent uranium produces efficient luminescence at relatively longer wavelength. Ropp [1] has reported that Sr_2WO_5 has a tetragonal structure, however no detailed structural study for this compound is reported.

In the present work, detailed structural and thermal study of Sr_2WO_5 has been carried out and the results are discussed. Structure of Sr_2WO_5 was refined using powder X-ray diffraction and neutron diffraction data. Thermal stability of the compound was studied using thermogravimetric analysis technique. Thermo physical properties such as thermal expansion and specific heat capacity of Sr_2WO_5 along with $SrWO_4$ and Sr_3WO_6 were also derived under identical experimental conditions using HTXRD and DSC techniques, respectively.

2. Experimental

$SrWO_4$, Sr_2WO_5 and Sr_3WO_6 were synthesized by solid state route, by reacting WO_3 with 1, 2 and 3 moles of $SrCO_3$, respectively. Reaction mixtures were heated at 1473 K for 10 h with intermittent grindings at 1073 and 1273 K. As $SrCO_3$ readily picks up moisture, it was preheated at 873 K for 4 h and stored in desiccators before use.

Formation of pure product phases was identified by XRD, using Rigaku Miniflex-600 X-ray diffractometer (Bragg Brentano geometry with θ-θ goniometer) with graphite monochromatised Cu $K\alpha_1$ radiation at λ=1.5406 Å at the scanning rate of 2° (2θ)/min. For structural study, powder XRD data of Sr_2WO_5 was collected in step scan mode between 2θ = 10 to 100° with step interval of 0.02° and counting time 4 sec. The room temperature powder neutron diffraction (ND) data was collected with the linear 5-PSD based powder diffractometer at 100 MW Dhruva Research Reactor, Trombay, Mumbai using neutrons of wavelength 1.2443 Å in the two-theta range of 10–110°. Rietveld refinement was carried out using FULLPROF program [25]. HTXRD data for $SrWO_4$, Sr_2WO_5 and Sr_3WO_6 were collected under vacuum (10^{-5}

mbar) on a STOE X-ray diffractometer using HDK-2.4 Buhler high temperature attachment from 298-1273 K. The experimental conditions and calibration of HTXRD instrument are discussed elsewhere in detail [26].

The structural and thermal stability of the compounds were checked by recording Thermogravimetric (TG) and Differential Thermal Analysis (DTA) curves simultaneously. Thermograms of the compounds were recorded on Mettler Thermoanalyzer (model:TGA/SDTA851^e/MT5/LF1600) in dry air from room temperature to 1273 K at the heating rate of 10 K min^{-1}. Around 100 mg sample was heated in alumina crucible (Vol. 150μL) with gas flow rate of 100 mL min^{-1}. All the weight changes were corrected for buoyancy correction, obtained under identical experimental conditions.

Heat capacity measurements of the compounds were carried out using a heat flux-type Differential Scanning Calorimeter (DSC, model number DSC 1/700 of M/s. Mettler Toledo GmbH, Switzerland) from 303 to 863 K. For measurement of heat capacity, classical three-step method was used for blank, sapphire and sample runs in continuous heating mode under identical experimental conditions. A thin disc of sapphire (SRM 720) was used as the heat capacity standard. Heat flow as a function of temperature was measured at the heating rate of 10 K min^{-1} in high purity argon atmosphere with a flow rate of 20 mL min^{-1}. Powder samples (120-150 mg) were loaded in 70 μL Pt crucible for heat capacity measurements. The experimental conditions are discussed in details elsewhere [27]. Average of six heat flow runs were taken for heat capacity measurements of Sr_2WO_5(s) and Sr_3WO_6 (s) and are within ± 2%.

3. Results and discussion

3.1. Structural study

Powder XRD patterns for the phases $SrWO_4$, Sr_2WO_5 and Sr_3WO_6 agreed well with the reported phases of the compounds and thereby confirming the formation of these phases. However, 2-3% phase impurity of $SrWO_4$ was observed in Sr_2WO_5 and Sr_3WO_6 compounds. As no structural data is available for Sr_2WO_5, structural study of Sr_2WO_5 has been carried out using powder XRD and ND data. Ba_2WO_5 was used as a starting model for refinemnt of Sr_2WO_5 structure [28]. Fullprof software was used for carrying out Rietveld refinement [25]. The profile

was fitted with Pseudo-Voigt profile function and the background was fitted with six parameters polynomial. Initially the scaling factor, sample displacement and background parameters were refined with the unit cell parameters to fit the observed X-ray diffraction data. Subsequently half width parameters and peak asymmetry correction were also included in the refinements. After getting a proper match in the profile model, the positional parameters and overall thermal parameters for Sr and W cations were refined. The refined model was than used for fitting the neutron diffraction data. The position parameters and overall thermal parameters of the lighter oxygen atoms were refined. The goodness of the refinements was observed by the residuals (R-values). The details of the various profile parameters and structural parameters are discussed below.

Sr_2WO_5 has orthorhombic crystal lattice with a space group Pnma (No. 62). Lattice parameters obtained from Rietveld refinement of the powder XRD data are: a = 7.2491(3) Å, b = 5.5488(2) Å, c = 10.8916(4) Å and volume = 438.1016(1) $Å^3$, which are comparable with those reported in ICDD card [29]. The density of Sr_2WO_5 mesured pyknometrically using toulene as a solvent ($\rho_{meas.}$=6.63 gm/cc) is comparable with the X-ray density ($\rho_{cal.}$=6.65 gm/cc) with 4 molecules per unit cell (Z=4). The XRD and ND Rietveld refinement plots for Sr_2WO_5 are shown in Fig. 1 [A] and [B], respectively. In figures 1A, reflections due to impurity phase $SrWO_4$ (2-3%) are observed at 2θ =17.96° and 27.64° and are shown by solid circles. The refined crystal structural parameters and bond lengths along with the average Bond Valance Sum (BVS) for Sr_2WO_5 are listed in Tables 1 and 2, respectively. The structure of Sr_2WO_5 is shown in Fig. 2 [A]. Structure contains distorted octahedra, which are linked by common corners and form infinite cis-bridged chains along the b- axis. These extended chains are further connected by the layers of Sr atoms as shown in Fig. 2 [B]. Sr atoms connect the WO_6 octahedra chains and form 10 co-ordinated sphenocorona with oxygen atoms from the adjacent layers. The average BVS calculated using VaList program for Sr is 2.01 and for tungsten is 6.08 matched well, with the expected oxidation states for these cations [30].

3.2. Thermal study

3.2.1. Thermal stability

TG curves of freshly prepared $SrWO_4$, Sr_2WO_5 and Sr_3WO_6 recorded in dry air did not show any weight change up to 1473 K. Moreover, the DTA does not show any indication of an endothermic or an exothermic peak. These observations confirmed the thermal as well as the structural stabilities of the compounds. During the structural study of Sr_3WO_6, King et al. [8] have stated that the high content of Sr in the compound and its sensitivity to moisture results in gradual decomposition of the material. In the present study also, it was observed that when Sr_2WO_5 and Sr_3WO_6 were left open in static air (average relative humidity ~ 70 % at 298 K), they were un stable and readily picked up moisture on storage. XRD patterns of freshly synthesized Sr_2WO_5 and Sr_3WO_6 along with XRD of their stored samples for different durations are shown in Fig. 3 and Fig. 4, respectively. It is clear from the XRD patterns in the stored Sr_2WO_5 and Sr_3WO_6 additional lines are due to the formation of $SrWO_4$. Sr_3WO_6 showed the X-ray lines of additional phase $Sr(OH)_2$, which could not be seen in the XRD pattern of stored Sr_2WO_5, probably because, the $Sr(OH)_2$ formed may be below the detection limit of XRD (~ 5 wt. %). To confirm the formation of $Sr(OH)_2$, thermogravimetric curves of $SrWO_4$, Sr_2WO_5 and Sr_3WO_6 stored in air for 80 days were recorded and shown in the Fig. 5. From the figure it can be confirmed that $SrWO_4$ is stable and did not show any weight change up to 1273 K. This is in agreement with the results reported by Krzmanc et al. [13]. However, Sr_2WO_5 and Sr_3WO_6 showed weight changes in two steps between 300 to 700 K and 800 to 1100 K. The first weight loss step is, due to the loss of moisture whereas the second step corresponds to the decomposition of strontium hydroxide to strontium oxide. The TG curves of 80 days stored Sr_2WO_5 and Sr_3WO_6 sample showed hydroxide weight loss of 0.55% and ~1.1%, respectively. Also, weight loss due to moisture present in the sample, is more in Sr_3WO_6 than in Sr_2WO_5. This may be explained on the basis of higher strontium content in Sr_3WO_6 as compared to that of Sr_2WO_5. Thus from XRD and TG studies it can be interpreted that on storage, Sr_2WO_5 and Sr_3WO_6 are picking up moisture and partially getting converted into -$SrWO_4$ and $Sr(OH)_2$. The partial conversion of Sr_2WO_5 and Sr_3WO_6 after picking up of moisture under ambient conditions can be given as:

$$Sr_2WO_5 + H_2O \leftrightarrows SrWO_4 + Sr(OH)_2 \quad (1)$$

$$Sr_3WO_6 + 2\,H_2O \leftrightarrows SrWO_4 + 2\,Sr(OH)_2 \quad (2)$$

The above equations reveal that the formation of hydroxide is double in the case of Sr_3WO_6 as compared to that of Sr_2WO_5.

To understand the thermal decomposition of $Sr(OH)_2$, the compound was prepared by mixing aqueous solutions of $Sr(NO_3)_2$ and NaOH in 1:1 molar proportion. The precipitate was dried with ethyl alcohol. The composition of the precipitate was ascertained from XRD and TG analysis. XRD analysis showed the composition of the precipitate as anhydrous $Sr(OH)_2$. TG curve of $Sr(OH)_2$ shown in Fig. 6 indicates the weight losses in three steps between 310 to 400 K, 720 to 880 K and 880 to 1040 K. The first weight loss step is due to the loss of loose moisture. The second and third steps showed decomposition of molten $Sr(OH)_2$ to SrO (Obs. weight loss = 14.34) which is in agreement with the calculated weight loss of 14.8% and also reported by Dinescua and Preda [31].

In order to get the quantitative data on the formation of $Sr(OH)_2$ during storage of Sr_2WO_5, synthetic mixtures of $SrWO_4$ containing 10 and 40 mol. % of $Sr(OH)_2$ were prepared and thermograms of the mixtures were recorded in dry air which are included in Fig. 6. As discussed above, $SrWO_4$ is a stable compound and does not pick up any moisture on storage. Thus, TG curves of synthetic mixtures of $SrWO_4$ and $Sr(OH)_2$ showed weight loss between 720 to 1200 K which corresponds to the decomposition of anhydrous strontium hydroxide to strontium oxide. The observed weight losses for both the compositions matched well with the expected weight loss and are given in Table 3.

3.2.2. Estimation of $Sr(OH)_2$ formation during storage of Sr_2WO_5

During the structural study of Sr_3WO_6 king et al. [8] have mentioned that the compound absorbs moisture as strontium is moisture sensitive which results in gradual decomposition of the compound. Since moisture sensitivity of Sr_3WO_6 is already reported, a systematic study was carried out for the evaluation of the sensitivity of Sr_2WO_5 towards moisture using XRD and thermogravimetric techniques. For this, a freshly prepared Sr_2WO_5 was exposed to static atmosphere having average relative humidity ~ 70 % at 298 K. XRD and thermograms of the stored samples were recorded after 0, 18, 80, 120 and 180 days. TG curves of stored samples indicate that the weight loss takes place in two steps due to the presence of loose moisture and decomposition of $Sr(OH)_2$. TG curves obtained by heating the stored Sr_2WO_5 in dry air are

shown in Fig. 7. The figure clearly indicates that as Sr_2WO_5 is stored for longer duration, the weight loss due to moisture as well as the decomposition of $Sr(OH)_2$ also increases. Thus, TG and XRD studies of that the stored Sr_2WO_5 consist of lose moisture and mixture of $SrWO_4$, $Sr(OH)_2$ and Sr_2WO_5 phases.

The quantitative data on formation of $Sr(OH)_2$ on storage of Sr_2WO_5 was obtained from thermogravimetric studies. Table 4 summarizes thermogravimetric data of freshly prepared and stored Sr_2WO_5 samples for 0 to 180 days. The weight loss in the temperature range of 800 to 1150 K was used to calculate the formation of hydroxide during storage. Pure anhydrous $Sr(OH)_2$ showed 14.34 % loss forming SrO as final product as given in Table 3. Assuming the stored samples as $Sr(OH)_2$, the expected weight loss (X) for complete conversion to SrO was calculated. By comparing the observed weight loss of stored samples (Y) with (X), the % of $Sr(OH)_2$ formed was calculated as [(Y)*100]/(X). Equation (1) clearly indicates that during partial decomposition of Sr_2WO_5, equal moles of $Sr(OH)_2$ and $SrWO_4$ are formed whose molecular weights are in 1:2.76 proportions. From the amount of $Sr(OH)_2$ formed, the weights of $SrWO_4$ was calculated. The quantity of unreacted Sr_2WO_5 can be obtained by subtracting amount of [$Sr(OH)_2$ + $SrWO_4$] from the weights of anhydrous samples. Table 4 clearly indicates that in Sr_2WO_5 the formation of $Sr(OH)_2$ increases from 0 to 4.8 wt. % on storage up to 180 days which is equivalent to 15 mole % of $Sr(OH)_2$. Fig. 8 shows the observed % weight loss of Sr_2WO_5 vs. number of days of storage at 298 K. From the figure it can be said that the moisture pick up is very fast initially and then gradually reaches to a saturation value with storage of time. The figure also shows that within 180 days the hydroxide formation reaches a maximum value. This study clearly indicates that properties of Sr_2WO_5 will degrade with storage time and thus special care needs to be taken to avoid the contact of moisture with the sample.

It was observed that stored Sr_2WO_5 and Sr_3WO_6 compounds when reheated at 1473 K, form respective pure tungstate compounds. This can be explained as, the stored Sr_2WO_5/Sr_3WO_6 on absorption of moisture gets partially converted to a mixture of $SrWO_4$ and $Sr(OH)_2$. This mixture, on heating above 1000 K, decomposes to SrO, which combines in-situ with $SrWO_4$ to form Sr_2WO_5/Sr_3WO_6. XRD patterns shown in Fig. 3 and 4 confirm the above observations.

3.3. Thermal expansion studies

As no data is available for thermal expansion behavior of Sr_2WO_5, the same has been studied in vacuum (10^{-5} mbar) from 298 to 1273 K using HTXRD technique. Fan et al. [7] have studied thermal expansion behavior of $SrWO_4$ single crystal up to 773 K using dilatometer. Thermal expansion behavior of Sr_3WO_6 has been studied by King et al. [8] using synchrotron based HTXRD. They have reported phase transitions in Sr_3WO_6 between 464 and 506 K, but have mentioned that the lattice parameters increases linearly up to 1373 K without anomalies at the transitions temperature. However, no thermal expansion coefficients are reported. Therefore, thermal expansion studies of $SrWO_4$, Sr_3WO_6 were also carried out in vacuum from ambient to 1273 K. Room temperature XRD data of $SrWO_4$, Sr_2WO_5 and Sr_3WO_6 were indexed on tetragonal, orthorhombic and triclinic systems, respectively. HTXRD patterns of all the three compounds recorded from ambient to 1273 K were similar except for the shift in the X-ray line positions to lower 2θ values, indicating the expansion of lattice with rise in temperature. Lattice parameter and unit cell volume of $SrWO_4$, Sr_2WO_5 and Sr_3WO_6 were plotted against the temperatures and are shown in Fig. 9 [A], [B] and [C], respectively. Percentage thermal expansion of lattice parameters and cell volumes were calculated using the formula,

$$\text{Expansion (\%)} = (a_T - a_{298}) \times 100 / a_{298} \quad (3)$$

Where, a_T and a_{298} represents the lattice parameter or volume at temperature T and at 298 K, respectively.

The variation in lattice parameter ′a′, ′b′, ′c′ and volume (Vol.) of the oxides were fitted to second order polynomial expressions of the form

$$a = x_1 + y_1T + z_1T^2 \quad (4)$$

$$b = x_2 + y_2T + z_2T^2 \quad (5)$$

$$c = x_3 + y_3T + z_3T^2 \text{ and} \quad (6)$$

$$\text{vol.} = x_4 + y_4T + z_4T^2 \quad (7)$$

where T denotes the absolute temperature in K. The coefficients x_1, y_1 and z_1, x_2, y_2 and z_2, x_3, y_3 and z_3 and x_4, y_4 and z_4 of the fitted equations of the lattice parameters a, b, c and vol., respectively against the temperature, T (K) for the three compounds are given in Table 5.

The axial (α_a) and volume thermal expansion coefficient (α_v) were derived from the equations ; $\alpha_a = (\Delta a_T/a_{298}) \times (1/\Delta T)$ and $\alpha_v = (\Delta v_T/v_{298}) \times (1/\Delta T)$, respectively where $\Delta a_T/\Delta v_T$ is the difference between lattice parameter/cell volume at any given temperature T (a_T/v_T) and lattice parameter/cell volume at room temperature (a_{298}/v_{298}); ΔT is the corresponding temperature difference. The average axial as well as volume thermal expansion coefficients for $SrWO_4$, Sr_2WO_5 and Sr_3WO_6 are given in Table 6.

3.4. Heat capacity measurements

Specific heat capacity of $SrWO_4$ has been already measured using DSC by Fan et al. [7]. Heat capacities of freshly prepared Sr_2WO_5(s) and Sr_3WO_6(s) samples were measured using heat flux type Differential Scanning Calorimeter (DSC) from 303-863 K. Averages of six runs were carried out. During collection of the Cp measurement data of Sr_2WO_5, first heating cycle showed two endothermic peaks at 362 and 423 K. The cooling cycle showed a single exothermic peak at 417 K. However, all subsequent heating and cooling cycles showed only a single peak at 423 and 417 K, respectively. It has been discussed earlier that Sr_2WO_5 is moisture sensitive, and thus the endothermic peak obtained during first heating cycle at 362 K can be assigned to the loss of moisture. In further heating cycles, the peak due to lose moisture was absent. The peak obtained at 423 K, observed in all heating cycles indicates structural phase transition in the compound. During cooling cycle, peak was obtained at 417 K, confirmed reversibility of the phase transition. Heating and cooling DSC curves obtained during 1st and 2nd cycle are shown in Fig. 10 [A]. ΔH of the phase transition of Sr_2WO_5 at 423 K was determined from DSC peak area measurement during heating and cooling cycles using indium (m.p = 429.7 K, ΔH fusion = 3.28 kJ/mol) and zinc (m.p = 692.7 K, ΔH fusion = 7.32 kJ/mol) as standards and was found to be 285 ± 15 J/mol. The low value of enthalpy of transition indicates that there is not much change in the structure during phase transition. The observed DTA and HTXRD studies also could not detect any phase transition. Multiple phase transitions have been reported for Sr_3WO_6 from 303 to 1373 K which were detected in temperature programmed synchrotron x-ray powder diffraction, neutron diffraction and electron diffraction [8]. It has been mentioned that room temperature triclinic phase transforms to monoclinic phase above 464 K without drastic change in structural parameters.

The values of heat capacity of Sr_2WO_5(s) or Sr_3WO_6(s) were calculated from heat flow signals measured by DSC using following relation:

$$C_p(T)_{sample} = \{(HF_{sample} - HF_{blank})/(HF_{ref.} - HF_{blank})\}*(M_{ref.}/M_{sample})*(C_p(T)_{ref.}) \quad (8)$$

where HF_{blank}, $HF_{ref.}$ and HF_{sample} represent heat flow during first (blank), second (reference) and third (sample) runs, respectively. $C_p(T)_{sample}$ and $C_p(T)_{ref.}$ are the heat capacities, and M_{sample} and $M_{ref.}$ are the molar masses of [Sr_2WO_5(s) or Sr_3WO_6(s)] and sapphire (s), respectively. Measured molar heat capacity data for Sr_2WO_5(s) or Sr_3WO_6(s) are given in Table 7 and plotted in Fig. 10 [B]. The fitted curves are also shown in the figure as solid lines. The inception in Fig. 10 [B] indicates a phase transition for anhydrous Sr_2WO_5 at 421 K and thus C_p data for the same was collected from 463 to 863 K.

The specific heat capacities of Sr_2WO_5 and Sr_3WO_6 fitted as a function of temperature in the form of $C_p = A + BT + C/T^2$ and are shown below:

Sr_2WO_5

$$C^o_{p,m}\,(J\cdot K^{-1}\cdot mol^{-1}) = 208.061\text{-}18.27\times10^{-3}\,(T/K)\text{-}48.80\times10^{5}(K/T)^2 \quad (463 \le T/K \le 863) \quad (9)$$

Sr_3WO_6

$$C^o_{p,m}\,(J\cdot K^{-1}\cdot mol^{-1}) = 240.282+5.86\times10^{-3}\,(T/K)\text{-}40.192\times10^{5}(K/T)^2 \quad (303 \le T/K \le 863) \quad (10)$$

The values of constants A, B and C are given in Table 6. As Sr_2WO_5 shows phase transition, C_p data for the same was collected from 463 K to 863 K. The inset shown in Fig. 10 [B] depicts the reversible phase transition in Sr_2WO_5. The relative standard deviations between observed and fitted values of heat capacity are in the range of 1-2 %.

4. Conclusions

Crystal structure of Sr_2WO_5 was derived from powder XRD and neutron diffraction data using Rietveld profile method. Structure consists of WO_6 octahedra forming infinite chains which are connected by the layers of SrO_{10} atoms. Compound picks up moisture and partially

getting converted to form $SrWO_4$ and $Sr(OH)_2$. Strontium hydroxide content increases with the storage of time and was estimated using thermogravimetric technique. Maximum 15 mol % of $Sr(OH)_2$ was formed on 180 days of storage. DSC study confirmed reversible phase transition in Sr_2WO_5 at 423 K with the enthalpy of transition 285 ± 15 J/mol. Thermal expansion and heat capacities of the compound were measured in the temperature range of 298-1273 K and 463-863 K, respectively. Thermal expansion of $SrWO_4$ and Sr_3WO_6 were also studied in vacuum and both compounds showed positive expansion from ambient to 1273 K.

References

[1] R.C. Ropp, Group 6 (Cr, Mo and W) alkaline earth compounds, Chapter10, Encyclopedia of alkaline earth compounds, Elsevier, The Netherlends (2013).

[2] B.S. Barros, A.C. deLima, Z.R. daSilva, D.M.A. Melo, S. Alves-Jr, Synthesis and photo luminescent behavior of Eu^{3+} doped alkaline-earth tungstates, J. Phys. Chem. Solids 73 (2012) 635–640.

[3] H.P. Barbosa, J. Kai, I.G.N. Silva, L.C.V. Rodrigues, M.C.F.C. Felinto, J.Holsa, O.L. Malta, H.F. Brito, Luminescence investigation of R^{3+}-doped alkaline earth tungstates prepared by a soft chemistry method, J. Lumin. 170 (2016) 736–742.

[4] H.M. Pask, J.A. Piper, Practical 580 nm source based on frequency doubling of an intracavity-Raman-shifted Nd:YAG laser, Opt. Commun.148 (1998) 285–288.

[5] Y.L. Huang, X.Q. Feng, Z.H. Xu, G.J. Zhao, G.S. Huang, Growth and spectra properties of Nd^{3+} doped $PbWO_4$ single crystal, Solid State Commun. 127 (2003) 1–5.

[6] D.S. Lee, K.H. Nam, D.D. Lee, Effect of substrate on NO^{2-}sensing properties of WO_3 thin film gas sensors, Thin Solid Films 375 (2000) 142–146.

[7] J. D. Fan, H. J. Zhang, J. Y. Wang, M. H. Jiang, R. I. Boughton, D. G. Ran, S. Q. Sun, H. R. Xia, Growth and thermal properties of $SrWO_4$ single crystal, J. App. Phys. 100 (2006) 063513.

[8] G. King, A.M. Abakumov, J. Hadermann, A.M. Alekseeva, M.G. Rozova, T. Perkisas, P.M. Woodward, G. Van Tendeloo, E.V. Antipov, Crystal structure and phase transitions in Sr_3WO_6, Inorg. Chem. 49 (2010) 6058–6065.

[9] M. Araba, A. L. Lopes-Moriyamaa, T. R. dos Santosa, C. P. de Souza, J. R. Gavarri, C. Leroux, Strontium and cerium tungstate materials $SrWO_4$ and $Ce_2(WO_4)_3$: Methane oxidation and mixed conduction, Cataly. Today 208 (2013) 35–41.

[10] F. Kang, Y. Hu, L. Chen, X. Wang, H. Wu, Z. Mu, Luminescent properties of Eu^{3+} in MWO_4 (M=Ca, Sr,Ba) matrix, J. Lumin. 135 (2013) 113–119.

[11] Z. Piskula, J. Czajka, K. Staninski, S. Lis, Luminescence properties of calcium tungstate activated by lanthanide (III) ions, J. Rare Earths 32 (2014) 221–225.

[12] Y. Li, Z. Wang, L. Sun, Z. Wang, S. Wang, X. Liu, Investigation of oxygen vacancy and photoluminescence in calcium tungstate nanophosphors with different particle sizes Y. Wang, Mater. Res. Bull. 50 (2014) 36–41.

[13] M. M. Krazmanc, M. Logar, B. Budic, D. Suvorov, Dielectric and microstructural study of the $SrWO_4$, $BaWO_4$ and $CaWO_4$ Scheelite Ceramics, J. Am. Ceram. Soc. 94 (2011) 2464–2472.

[14] D.S. Perez, D. Errandonea, P.R. Hernandez, A. Munoz, R.L. Perales, A. Polian, Y. Meng, Polymorphism in strontium tungstate $SrWO_4$ under quasi-hydrostatic compression, Inorg. Chem. 55 (2016) 10406–10414.

[15] P. Botella, R.L. Perales, D. Errandonea, A. Polian, P. R. Hernandez, A. Munoz, High pressure Raman scattering of $CaWO_4$ up to 46.3 GPa: Evidance of a new high-pressure phase, Inorg. Chem. 53 (2014) 9729–9738.

[16] R. Vilaplana, R. L. Perales, O. Gomis, D. Errandonea, Y. Meng, Quasi-hydrostatic X-ray powder diffraction study of the low– and high–pressure phases of $CaWO_4$ up to 28 GPa, Solid State Sci. 36 (2014) 16–23.

[17] O. Gomis, J. A. Sans, R. L. Perales, D. Errandonea, Y. Meng, J. C. Chervin, A. Polian, Complex high-pressure polymorphism of barium tungstate, Phy. Rev. B 86 (2012) 054121.

[18] J.C. Grivel, P. Norby, Subsolidus phase relations of the SrO–WO_3–CuO system at 800°C in air, J. Alloys Compd. 513 (2012) 304–309.

[19] E. Gurmen, E. Daniels, J.S. King, Crystal structure refinement of $SrMoO_4$, $SrWO_4$, $CaMoO_4$, and $BaWO_4$ by neutron diffraction, J. Chem. Phys. 55 (1971) 1093–1097.

[20] D. Christofilos, S. Ves, G. A. Kourouklis, Pressure induced phase transitions in alkaline earth tungstates, Phys. Stat. Sol. (b) 198 (1996) 539–544.

[21] P.Goel, R. Mittal, S. L. Chaplot, A. K. Tyagi, Lattice dynamics of strontium tungstate, Pramana J. Phys. 71 (2008) 1135–1139.

[22] V.A Levitski, Y.Y Scolis, Thermodynamics of double oxides I. Galvanic-cell study of strontium tungstates and aluminates, J. Chem. Thermodyn. 6 (1974) 1181–1190.

[23] X. Zhao. Y. Ding, Z. Li, T. Yu, Z. Zou, An efficient charge compensated red phosphor Sr_3WO_6: K^+, Eu^{3+} – For white LEDs, J. Alloys Compd. 553 (2013) 221–224.

[24] G. Blasse, G.P.M. van den Heuvel, Uranium luminescence in di-alkaline-earth tungstates (Me_2WO_5), J. Lumin. 8 (1974) 406–414.

[25] J. Rodriguez-Carvajal, FULLPROF 2000 version 1.6, Laboratoire Leon Brillouin, Gif sur Yvette, France, (2000).

[26] Meera Keskar, K. Krishnan, N.D. Dahale, Thermal expansion studies on $Th(MoO_4)_2$, $Na_2Th(MoO_4)_3$ and $Na_4Th(MoO_4)_4$, J. Alloys Compd. 458 (2008) 104–108.

[27] Meera Keskar S. Dash, N.D. Dahale, K. Krishnan, S.K. Sali, Phase study in $SrO–UO_3–MoO_3$ system, J. Nucl. Mater. 434 (2013) 367–374.

[28] L.M. Kovba, L.N. Lykova, V.L. Balashov, A.L. Kharlanov, Crystal structure of Ba_2WO_5, Koordinatsionnaya Khimiya (=Coordination Chemistry (USSR)) 11 (10) (1985) 1426–1429.

[29] PDF Card Nos. 25-0810, International Centre for Diffraction Data, Newtown Square, USA.

[30] A.S. Wills, VaList, Program available from www.ccp14.ac.uk

[31] R. Dinescu, M. Preda, Thermal decomposition of strontium hydroxide, J. Thermal Anal. 5 (1973) 465–473.

Table 1

Crystal structure parameters for Sr_2WO_5 using X-ray and neutron diffraction data.

Lattice Parameters: a= 7.2491(3) Å, b= 5.5488(2) Å, c= 10.8916(4) Å, V= 438.10(3) $Å^3$

Space group: Pnma (No. 62)

XRD :R_p (%) = 8.8, R_{wp} (%) = 13.3, R_f-factor (%) = 3.11, GoF (χ^2) =1.71

Neutron: R_p(%) = 3.46, R_{wp} (%) = 4.43, R_f-factor (%) = 4.96, GoF (χ^2) = 4.4

Atom	Site	x	y	z	Biso($Å^2$)	Occupancy	BVS*
Sr1	4c	0.3140(6)	0.25	0.9143(4)	0.68(4)	1	1.882
Sr2	4c	0.0163(5)	0.25	0.2179(4)	0.65(4)	1	2.144
W	4c	0.1882(3)	0.75	0.0666(2)	0.13(8)	1	6.082
O1	4a	0	0.5	0	1.58(9)	1	2.008
O2	4c	0.0413(9)	0.75	0.2021(5)	1.99(2)	1	2.044
O3	4c	0.2759(7)	0.75	0.8992(5)	0.95(8)	1	2.042
O4	8d	0.3364(5)	-0.0007(1)	0.1134(3)	1.85(7)	1	2.007

Note: The refinement of crystal structure was done by initially refining the lattice parameters, atomic positions and thermal parameters Biso of heavy elements (Sr and W) using XRD data. The obtained model was then used for the refinement of the neutron diffraction data, where refinement of atomic positions and thermal parameters of lighter atom oxygen was taken into consideration.

* **B**ond **V**alance **S**um (BVS) was calculated using VaList program [26].

Table 2

Bond length and bond angle for Sr_2WO_5.

Bond	Bond length (Å)	Bond	Bond length (Å)	Bond	Bond length (Å)
Sr1-O1	2.824(4)	Sr2-O1	2.751(4)	W-O1	2.077(2)
Sr1-O1	2.824(4)	Sr2-O1	2.751(4)	W-O1	2.077(2)
Sr1-O2	2.87(2)	Sr2-O2	2.786(2)	W-O2	1.82(2)
Sr1-O2	2.54(2)	Sr2-O2	2.786(2)	W-O3	1.93(2)
Sr1-O3	2.793(3)	Sr2-O3	2.47(3)	W-O4	1.824(2)
Sr1-O3	2.793(3)	Sr2-O3	2.48(3)	W-O4	1.824(2)
Sr1-O4	2.581(2)	Sr2-O4	2.935(2)	<W-O>	1.9254
Sr1-O4	2.903(2)	Sr2-O4	2.648(2)		
Sr1-O4	2.903(2)	Sr2-O4	2.935(2)		
Sr1-O4	2.581(2)	Sr2-O4	2.648(2)		
<Sr1-O>	2.7612	<Sr2-O>	2.7196		

Bond angles <Oi-W-Oi> in WO_6 octahedra	O1	O2	O3	O4
O1	83.82(8)	84.2(1)	83.46(2)	88.7(8)
O2	84.2(1)			96.78(9)
O3	83.46(2)			94.02(8)
O4	88.7(8)	96.78(9)	94.02(8)	98.66(5)

WO_6 bond angle variance = 35.7522 deg^2

Table 3

Thermogravimetric data of pure $Sr(OH)_2$ and synthetic mixtures of $Sr(OH)_2$ + $SrWO_4$.

Sr. No.	Composition	Wt. of sample (mg)	Temp range (K)	Wt. loss (%) Obs.	Cal
1	$Sr(OH)_2$	59.17	760-1040	14.34	14.80
2	$0.1Sr(OH)_2 + 0.9SrWO_4$	89.42	820-1190	0.55	0.57
3	$0.4Sr(OH)_2 + 0.6SrWO_4$	76.86	712-1220	2.70	2.88

Table 4

Thermogravimetric data of Sr_2WO_5 after storage for different time interval in static air at 298 K and average relative humidity ~ 70 %.

Sr. No.	Period of storage (d)	Wt. of sample * (mg)	Temp range (K)	Wt. loss (%)	Wt. (%)			Compositions of stored compound
					$Sr(OH)_2$	$SrWO_4$	Sr_2WO_5	
1	0	363.3	-	0	0	0	363.3	Sr_2WO_5
2	18	100.98	773-973	0.34	2.30	6.50	91.20	0.84 Sr_2WO_5+0.08$SrWO_4$ + 0.08$Sr(OH)_2$
3	80	134.98	800-1000	0.52	3.61	9.96	81.43	0.76 Sr_2WO_5+0.12$SrWO_4$ + 0.12$Sr(OH)_2$
4	120	121.56	800-1053	0.63	4.36	12.03	83.61	0.72 Sr_2WO_5+0.14$SrWO_4$ + 0.14$Sr(OH)_2$
5	180	248.13	800-1123	0.69	4.80	13.25	81.90	0.70 Sr_2WO_5+0.15$SrWO_4$ + 0.15$Sr(OH)_2$

***** Weight of anhydrous sample

Table 5

Coefficients of the second order polynomial equations a(x1, y1, z1), b(x2, y2, z2), c(x3, y3, z3) and vol. (x4, y4, z4) used to fit the lattice parameters a, b, c and vol. against temperature, T (K) for $SrWO_4$, Sr_2WO_5 and Sr_3WO_6.

Compd.	x_1	y_1 ($\times10^{-5}$)	z_1 ($\times10^{-9}$)	x_2	y_2 ($\times10^{-5}$)	z_2 ($\times10^{-9}$)	x_3	y_3 ($\times10^{-5}$)	z_3 ($\times10^{-9}$)	x_4	y_4 ($\times10^{-5}$)	z_4 ($\times10^{-9}$)
$SrWO_4$	5.4122	1.2629	27.079	5.4122	1.2629	27.079	11.8421	24.912	35.520	346.923	873	4804
Sr_2WO_5	7.2264	6.5144	49.794	10.8605	15.1593	-3.3625	5.5221	7.7580	4.7037	433.289	1509	3554
Sr_3WO_6	10.092	5.7229	28.618	17.600	29.602	64.534	11.8010	8.5138	7.4623	1701.462	3973	24072

Table 6

Average thermal expansion coefficients (obtained in vacuum) and C_p data (collected in argon atmosphere) for $SrWO_4$, Sr_2WO_5 and Sr_3WO_6.

Compd.	Average thermal expansion coefficient [$\times 10^{-6}$] K^{-1}				*C_p ($J\ K^{-1}\ mol^{-1}$)		
	α_a	α_b	α_c	$\alpha_{vol.}$	A	B	C
$SrWO_4$	7.06	7.06	22.0	35.81	-	-	-
Sr_2WO_5	12.87	10.06	14.07	37.00	208.061	-18.27×10^{-3}	-48.80×10^{-5}
Sr_3WO_6	8.43	20.80	6.94	36.97	240.282	5.86×10^{-3}	-40.192×10^{-5}

*$C_p = A + BT + C/T^2$

Table 7

Heat Capacity data for Sr_2WO_5(s) and Sr_3WO_6(s)

Sr_2WO_5		Sr_3WO_6	
T/K	$C^o_{p,m}(T)$/J.K^{-1}.mol^{-1}	T/K	$C^o_{p,m}(T)$/J.K^{-1}.mol^{-1}
463.16	177	303.16	193.31
483.16	178	323.16	206.54
503.16	178.94	343.16	210.53
523.16	180.27	363.16	213.8
543.16	181.1	383.16	216.51
563.16	181.9	403.16	218.84
583.16	182.53	423.16	220.97
603.16	183.02	443.16	222.62
623.16	183.37	463.16	224.21
643.16	183.52	483.16	225.79
663.16	183.39	503.16	227.05
683.16	184.6	523.16	228.3
703.16	185.5	543.16	229.21
723.16	186.8	563.16	230.22
743.16	187.72	583.16	231.2
763.16	188.13	603.16	232.17
783.16	188.06	623.16	232.93
803.16	187.53	643.16	233.56
823.16	186.12	663.16	233.91
843.16	184.32	683.16	234.73
863.16	181.53	703.16	237.37
		723.16	239.18
		743.16	240.32
		763.16	241.17
		783.16	241.54
		803.16	242.01
		823.16	240.25
		843.16	236.91
		863.16	233.82

Captions of the Figures

Fig. 1. Rietveld refinement plots for [A] powder X-ray diffraction data; [B] Neutron diffraction data of Sr_2WO_5. Iobs., Ical., difference (Iobs. – Icalc.) and Bragg reflection positions has been shown in red, black, blue and green colours, respectively. Blue solid circles indicate XRD lines of impurity phase $SrWO_4$.

Fig. 2. [A] Crystal structure of Sr_2WO_5, color code: Sr-Green, W-Black, O-Red; [B] WO_6 octahedral zig-zag chain along b-axis.

Fig. 3. XRD patterns of Sr_2WO_5 freshly prepared [A], stored in air for 120 days [B], 180 days [C] and reheated at 1473 K [D]; ′+′ =X-ray lines due to $SrWO_4$.

Fig. 4. XRD of Sr_3WO_6, freshly prepared [A], stored in air for 80 days [B] and reheated at 1473 K [C]; ′+′ and # represent X-ray lines due to $SrWO_4$ and $Sr(OH)_2$, respectively.

Fig. 5. Thermogravimetric (TG) curves of 80 days stored $SrWO_4$, Sr_2WO_5 and Sr_3WO_6.

Fig. 6. TG curves of pure $Sr(OH)_2$ [A], synthetic mixtures of 0.1 $Sr(OH)_2$ + 0.9 $SrWO_4$ [B] and 0.4 $Sr(OH)_2$ + 0.6 $SrWO_4$ [C].

Fig. 7. Thermogravimetric curves of Sr_2WO_5 stored for different duration of time.

Fig. 8. Weight loss % due to decomposition of $Sr(OH)_2$ vs No. of days Sr_2WO_5 stored in static atmosphere.

Fig. 9. Variations of unit cell parameters and cell volume with temperature for $SrWO_4$ [A], Sr_2WO_5 [B] and Sr_3WO_6 [C].

Fig. 10. [A] DSC curve obtained during heating of Sr_2WO_5 from 300 K to 523 K and [B] heat capacity (C_p) of Sr_2WO_5 and Sr_3WO_6. Inset shows phase transition in Sr_2WO_5.

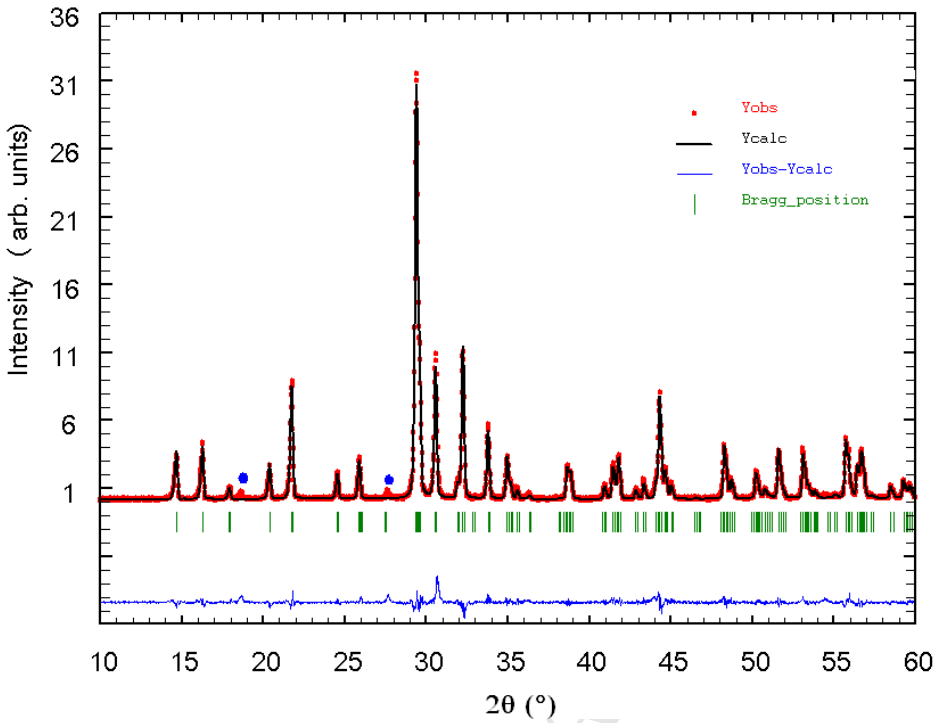
Intensity (arb. units)
36
31
26
21
16
11
6
1
Yobs
Ycalc
Yobs-Ycalc
Bragg_position
10
15
20
25
30
35
40
45
50
55
60
2θ (°)

[A]

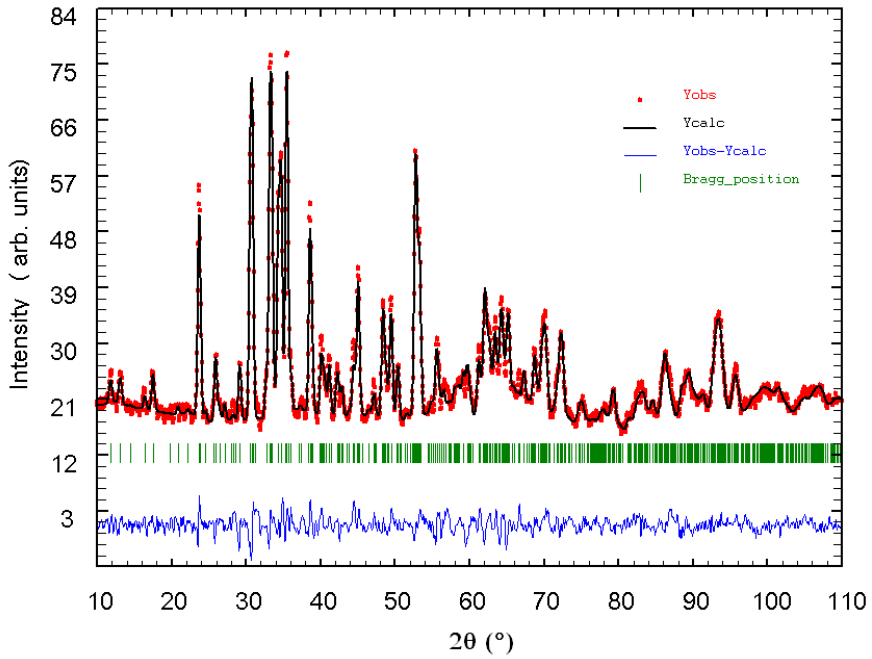
Intensity (arb. units)
84
75
66
57
48
39
30
21
12
3
Yobs
Ycalc
Yobs-Ycalc
Bragg_position
10
20
30
40
50
60
70
80
90
100
110
2θ (°)

[B]

Fig. 1.

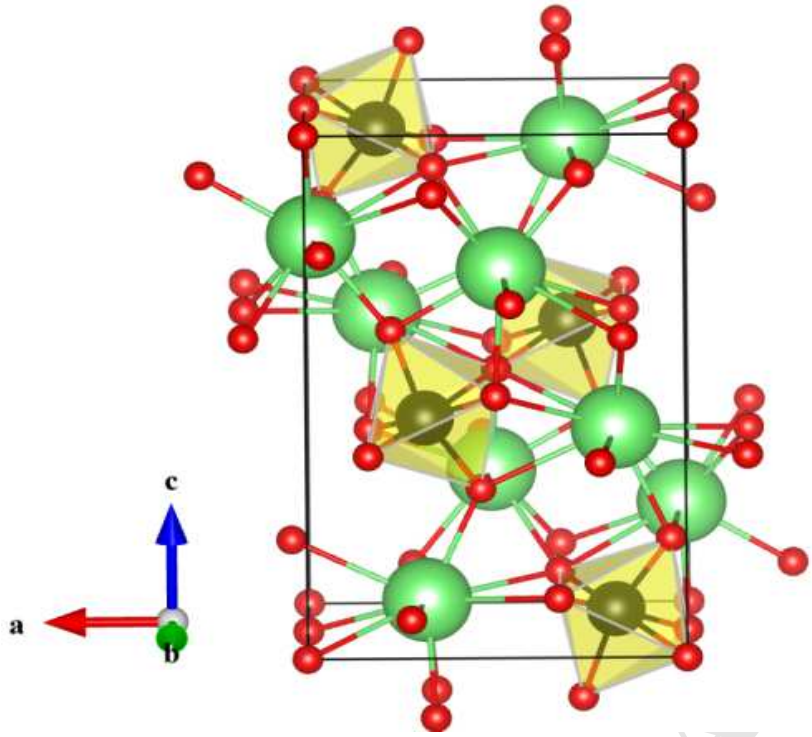

[A]

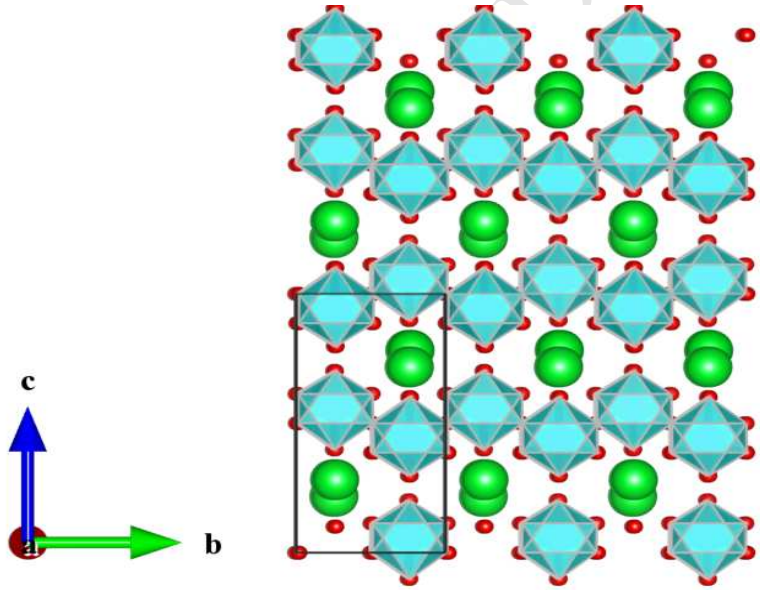

[B]

Fig. 2.

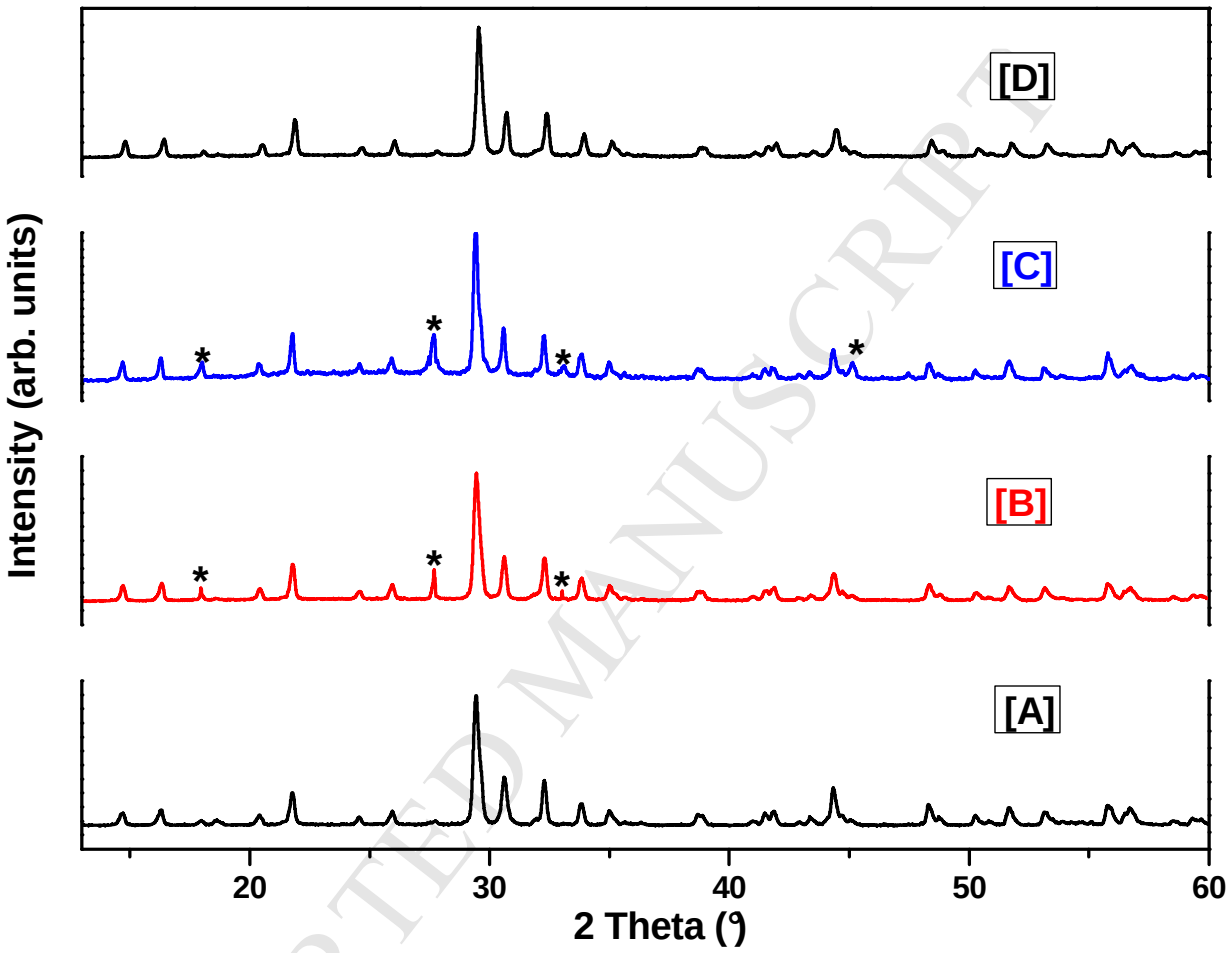

Fig.3

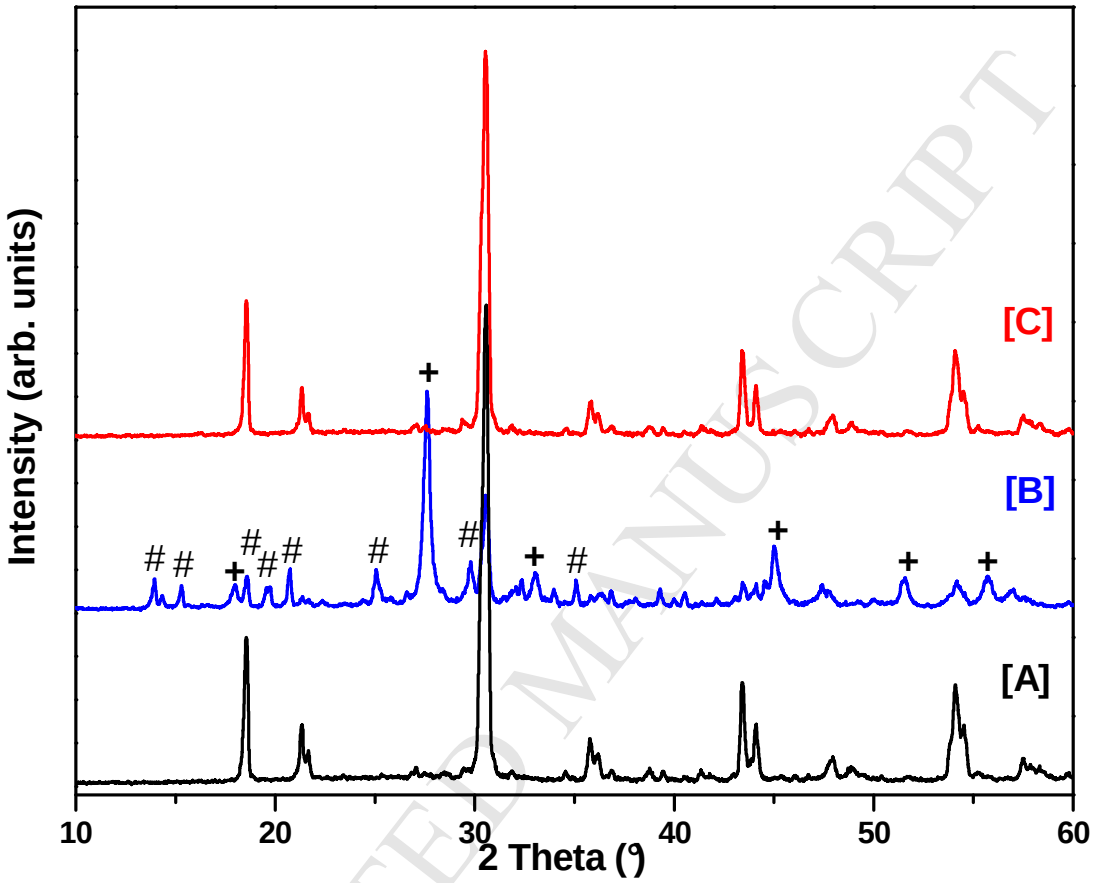

Fig. 4.

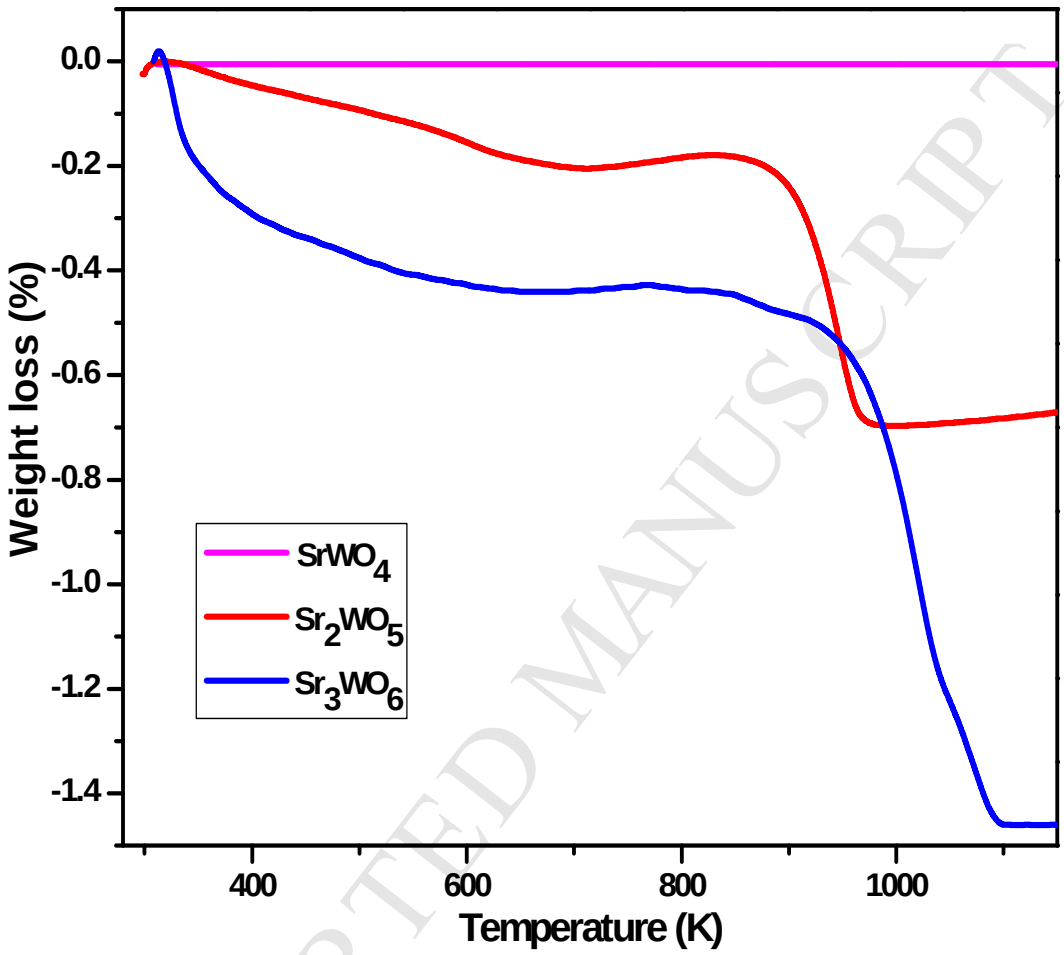

Fig. 5.

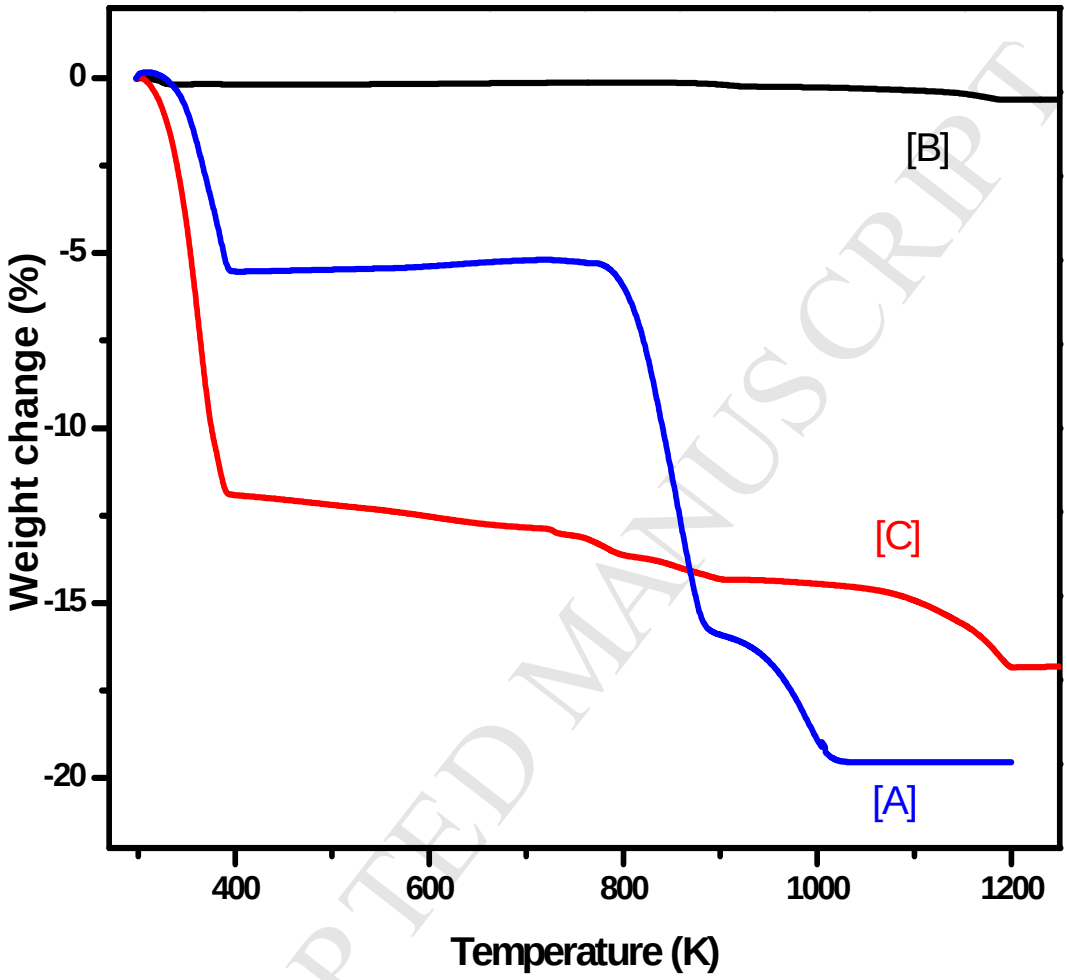

Fig. 6

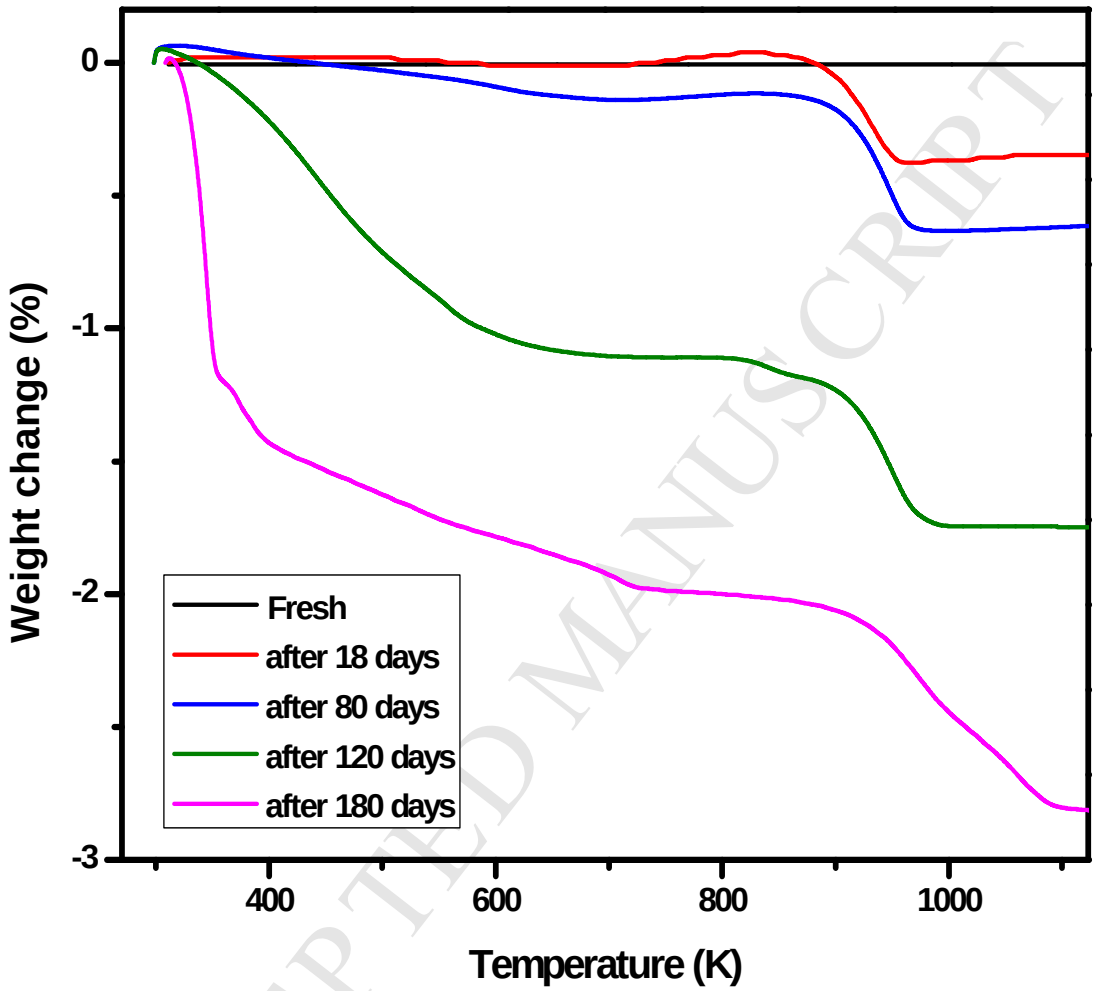

Fig. 7.

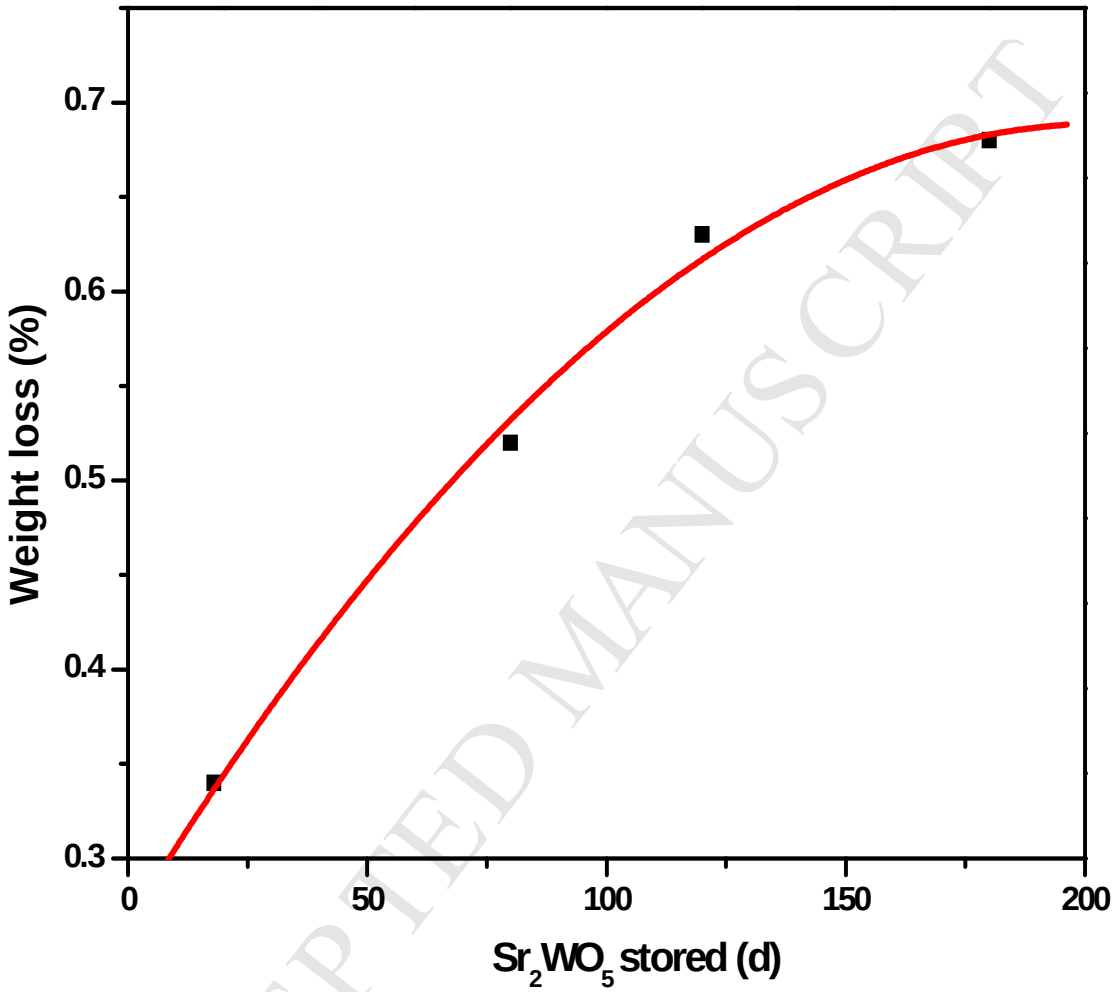

Fig. 8.

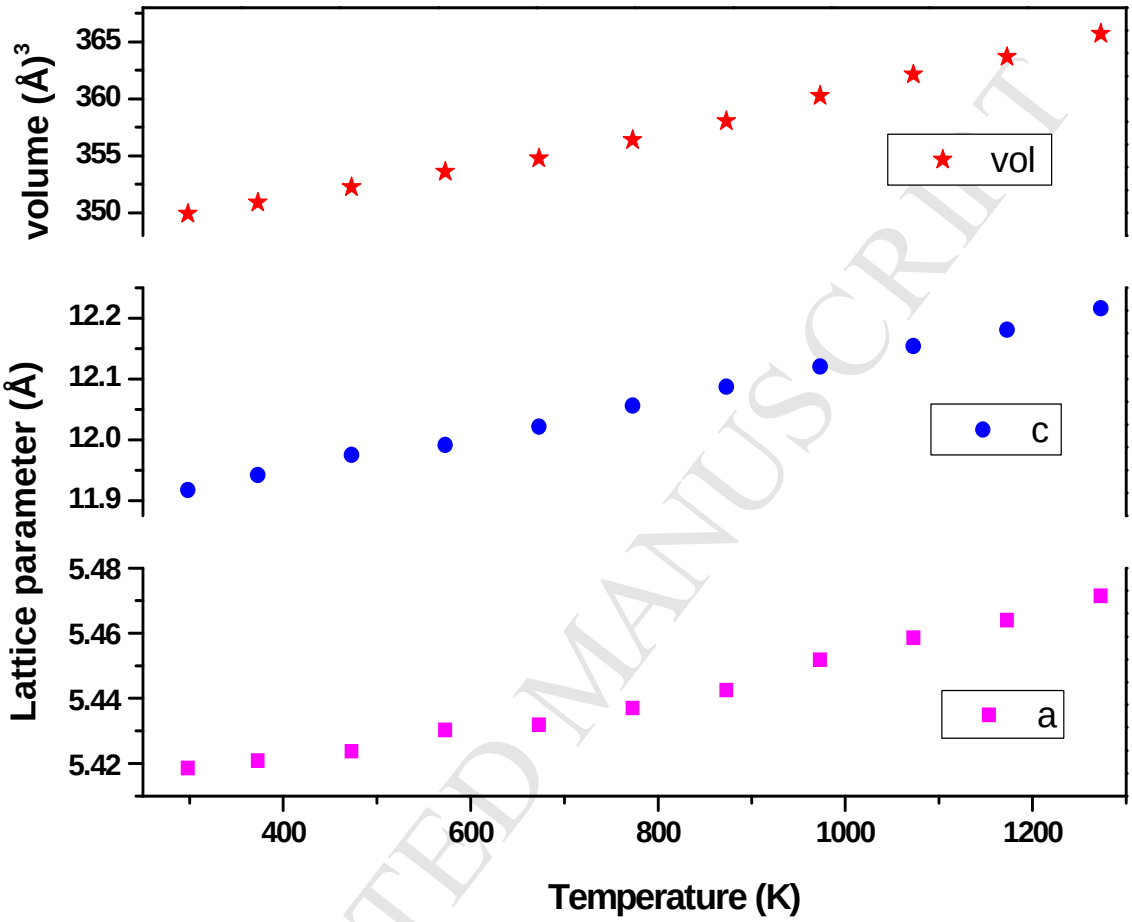

Fig. 9 [A]

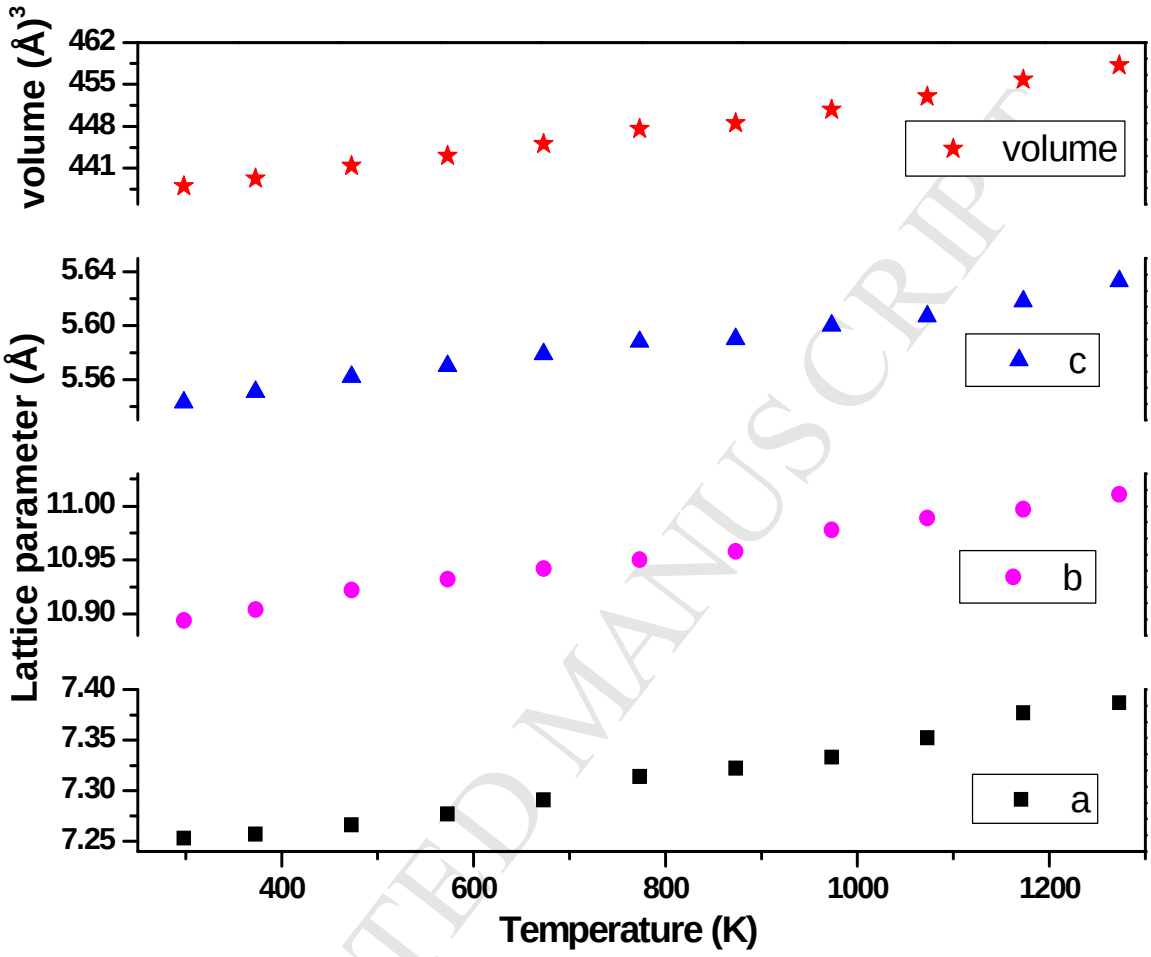

Fig. 9 [B]

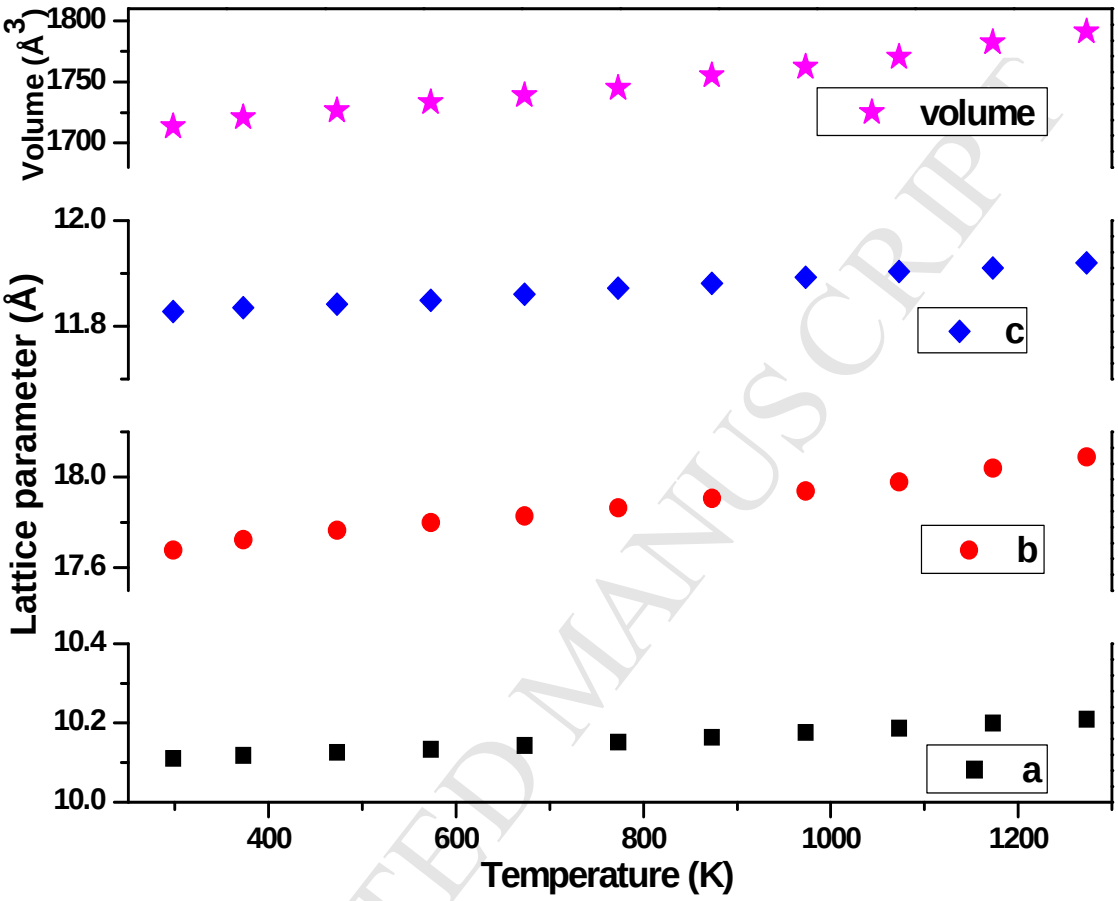

Fig. 9 [C]

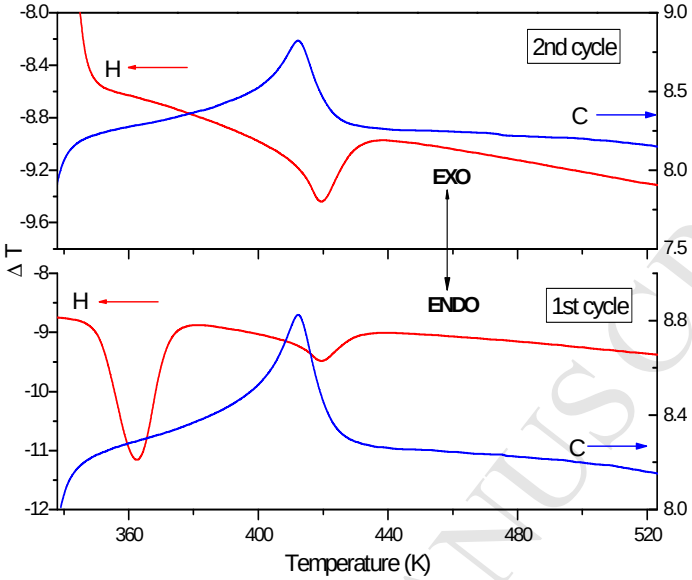

[A]

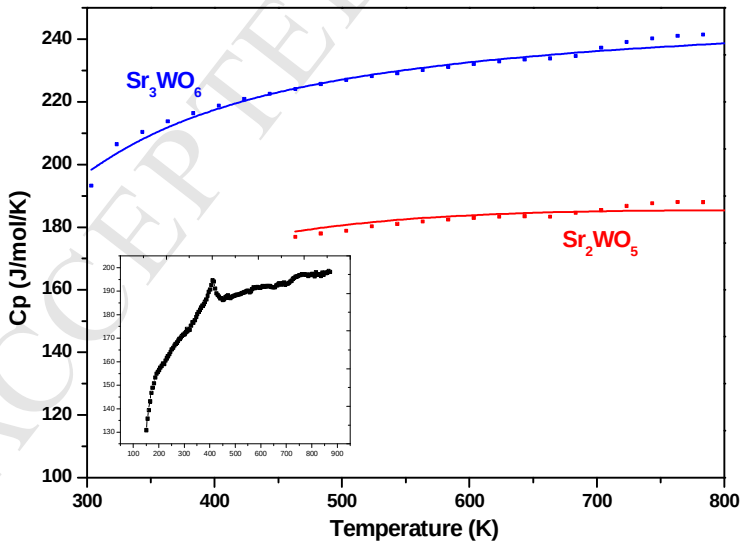

[B]

Fig. 10

Highlight of work

- **Crystal structure of Sr_2WO_5 was derived using XRD, neutron diffraction data.**
- **Thermal stability of the compound was studied.**
- **On storage, Sr_2WO_5 picks up loose moisture to give a mixture of $Sr(OH)_2$ and $SrWO_4$.**
- **Thermo physical properties of Sr_2WO_5 and Sr_3WO_6 were determined.**